Tension Reduction between Planck data and LSS by Dynamical Dark Energy Model

Aghileh Sadat Ebrahimi and Majid Monemzadeh **, Hossein Moshafi and Seyed Mohammad Sadegh Movahed*

Abstract

In this paper, we consider the dynamical dark energy model (Feng model) to reveal the discrepancy between CMB and LSS data raised by ΛCDM model. In order to constrained free parameters, we utilize two combined sets namely the *Planck* TT 2015+Pol+BAO and the WL+RSD. We find that, there is a tension between the best fit values for both σ_8 and H_0 derived by the early and late time observations in the context of ΛCDM model, while the mentioned discrepancy is alleviated in the Feng model. Two dimensional likelihood analysis demonstrate that including dynamical dark energy model alleviates $H_0 - \Omega_m$ and $\sigma_8 - \Omega_m$ tension from 2σ to 1σ confidence level compared to that of given for ΛCDM. Besides these, the models satisfy $f\sigma_8$ data in $0 < z < 0.4$ redshift bin but for $z > 0.4$, the models behave differently rather than data for both data sets.

Keywords: Dynamical Dark Energy Models, Tension, Structure Formation.

2019 Mathematics Subject Classification: Statistic , Numerical solution.

1   Introduction

The discovery of cosmic acceleration, challenges our understanding of the standard model of gravity and particle physics. The nature of late time acceleration of the

universe is still unknown and it is one of the fundamental enigmas and central challenges for theoretical cosmology. The simplest dark energy model, the cosmological constant (CC), is the first well-known possibility but it has two deeply realized problems: The Cosmological Constant Problem and the Coincidence Problem [1]. Hence two different theoretical attempts exist to explain the cosmic acceleration. The first approach is construction of dark energy as a hypothetical exotic component explanation such as quintessence [2], non canonical scalar field (k-essence) [3], phantom [4], coupled dark energy [5], running vacuum models as coupled dark energy [6] and other probable properties. The second approach is modification of gravity which allows the cosmic acceleration without any exotic component such as f(R) gravity [7, 8] , scalar-tensor theories[9, 10] and other probable properties.

Cosmological Constant has a constant equation of state $w = -1$. On the other hand, observations demonstrate that dark energy equation of state slightly favorite $w < -1$. However, deviation from cosmological constant enables us to construct new models such as dynamical dark energy (DDE) which its prediction will be detectable at the precision of future observations.

However, when we consider dynamical dark energy, we should attend its dynamical character not only in the background but also in the growth of structures. Hence, perturbation will be able to distinguish between cosmological constant and variable dark energy scenario and detecting either $w \neq -1$ or $\frac{dw}{dt} \neq 0$ would rule out cosmological constant as well.

Both Cosmic Microwave Background (CMB) and large scale structure (LSS) probes are tools for investigation of the Universe in early and late time and use to constrain the cosmological parameters. CMB constraints matter content of the Universe and its geometry. Hence, when combined with low redshift data such as Baryonic Acoustic Oscillations (BAO) and Weak Lensing (WL), is probing for dark energy (DE) models. Also, DE caused the secondary anisotropy on CMB which is sensitive to the different amount of potential and known as Integrated Sachs-Wolfe (ISW) effect. The detection of any ISW effect provides strong physical evidence for the existence of dark energy, and can be used to measure its equation of state [11].

Furthermore, LSS provides powerful tools for probing DE. The normalized σ_8, variance of matter fluctuations in the $8h^{-1}Mpc$ sphere, is sensitive to DE. This scale is inside the horizon and fluctuations are still linear but σ_8 is model-dependent and it also depends on galaxy bias [12]. Hence, it leads to the introduction of linear growth factor f which is base on peculiar velocities obtained from Redshift Space Distortion (RSD) measurements [13]. RSD is matter tracer in galaxy redshift surveys that measuring $f\sigma_8$ which is sensitive to DE models and galaxy bias independent [14]. Also, instead of looking for growth factor by numerically solving perturbed equations, the growth index γ can be used as a signature of dark energy and modified gravity [15].

At last scattering surface, Universe consists of a hot plasma of tightly coupled photons and baryons, competing of gravity and pressure sets up oscillations on photons fluid. So, acoustic wave in primordial plasma cause fluctuation in the

density of visible matter which called BAO and can be effected on large-scale structures through expanding the Universe and also can constraint DE models. Weak gravitational lensing is an important probe of the dark side of the Universe. It provides a way to map the distribution of dark matter around galaxies, clusters of galaxies on cosmological scales. In addition, lensing distortions measurement of the shapes of distant galaxies is a powerful probe for late time acceleration and DE properties [16]

There is a discrepancy between CMB measurements as large-scale data and those from LSS as small-scale within ΛCDM model. The level of agreement between weak lensing from CanadaFranceHawaii Telescope Lensing Survey (CFHTLenS) and Planck shows that the marginalized $\Omega_m - \sigma_8$ plane in 95 percent confidence level of the contour plot, CFHTLenS and CMB just only touch [17] and appear discrepancy between measurement of σ_8 using two data sets. It is shown that considering massive neutrino decreases tension from 2.5σ to 1.6σ [18]. Furthermore, it is shown that running vacuum model could effect on the tension and the central value of σ_8 for running vacuum model is 8.4% smaller than ΛCDM model and it relaxing the tension [19] Several attempts have been done to distinguish the discrepancy between these two data sets [20]. Also, non-relativistic dark matter or coupling dark matter to radiation is an interesting scenario which can reduce the tension [21, 22]. Also, the tension between the mentioned data is even more in $H_0 - \Omega_m$ two-dimensional contour plot [18].

In this research, we consider DDE as an important component to decrease this discrepancy of large and small-scale observation. In the next, we discuss scalar perturbations and dynamical model of dark energy, In chapter 3 we report data sets used in this paper. In chapter 4, we consider results and discussion. In chapter 5 we report the conclusion remarks.

2   Theoretical Notice

In order to clarify dark energy effects on structure formation in the theoretical framework, we will discuss the evolution of scalar perturbations, matter power spectrum and σ_8 in this section.

2.1   Scalar Perturbations

We consider line element for study the perturbations evolution of CDM in the present of dynamical dark energy (DDE) as:

$$ds^2 = a^2(\eta)\{-(1+2\psi)d\eta^2 + (1+2\phi)dx^i dx^j\}, \tag{1}$$

we are working in Newtonian gauge or longitudinal gauge, which influences on the perturbations especially on scales larger than Hubble horizon $k \leq aH$. On much smaller scales the choice of gauge is less important and observables are independent of gauge choice [23]. Where a is scale factor, η is conformal time ,

ϕ and ψ are variables describing scalar metric perturbations and known as gauge invariant Bardin potential [24]. Hence Einstein perturbed Eqs. and perturbed continuity fluid Eq. with vanishing anisotropy stress, for each mode leads to [24]:

$$k^2\phi + 3\mathcal{H}(\phi' - \mathcal{H}\psi) = 4\pi Ga^2\rho\delta \tag{2}$$

$$k^2\phi' - \mathcal{H}\psi = 4\pi Ga^2(1+\omega)\phi\theta \tag{3}$$

$$\psi = -\phi \tag{4}$$

$$\phi'' + 2\mathcal{H}\phi' + \mathcal{H}\psi' - (\mathcal{H}^2 + 2\mathcal{H}')\psi = 4\pi Ga^2 c_s^2\rho\delta \tag{5}$$

$$\delta' + 3\mathcal{H}(c_s^2 - w)\delta = -(1+w)(\theta + 3\phi') \tag{6}$$

$$\theta' + \left[\mathcal{H}(1-3w) + \frac{w'}{1+w}\right]\theta = k^2(\frac{c_s^2}{1+w}\delta + \psi) \tag{7}$$

where prime denotes differentiation respect with conformal time, $\delta = \frac{\delta\rho}{\rho}$ is density contrast, w is equation of state of fluid, c_s^2 is sound speed and $\theta = i\mathbf{k}.\mathbf{v}$ is velocity dispersion.

2.2   Matter Power Spectrum and σ_8

Density contrast described by the matter power spectrum which is Fourier transformation of matter correlation function. According to the linear theory on the large scales, gravity competes with cosmic expansion and structures grow. On small-scales, gravitational collapse is non-linear and can only computed correctly using N-body simulation. But at enough large scales, the perturbations are linear and can describe linear perturbation theory.

The most popular assumption is that the primordial fluctuations were distributed according to the homogeneous Gaussian random process which comes from the simple model of inflation [25]. Under this assumption all of the statistic information is encoded in the power spectrum. The power spectrum is given by $P(k) = k^n T^2(k)D^2(a)$, where $D(a)$ is the scale independent linear growth factor, $T(k)$ is the CDM transfer function and $n \simeq 0.9671$ following the recent reanalysis of the Planck data. For $T(k)$, we use the transfer function [26] is given by:

$$T(k) = C_q \left[1 + 3.89q + (16.1q)^2 + (5.46q)^3 + (6.71q)^4\right]^{-1/4}, \tag{8}$$

where $C_q = \frac{\ln(1+2.34q)}{2.34q}$ and $q \equiv \frac{k}{\Gamma}$. Here Γ is the shape parameter , given according to:

$$\Gamma = \Omega_m^0 \tilde{h} \exp(-\Omega_b^0 - \sqrt{2\tilde{h}}\Omega_b^0/\Omega_m^0), \tag{9}$$

the value of Γ, which is kept constant throughout the model fitting procedure, is estimated using the Planck results namely, $\Omega_b^0 = 0.02233 \pm 0.00015\tilde{h}^{-2}, \tilde{h} = 0.67$ and $\Omega_m^0 = 0.3147 \pm 0.0074$. The transfer function can use in present of dynamical dark energy models as well as cosmological constant. [27]

Also, the root mean square fluctuations of the linear density field on mass scale M_h is :

$$\sigma(M_h, z) = \left[\frac{D^2(z)}{2\pi^2} \int_0^\infty k^2 P(k) W^2(kR) dk \right]^{1/2}. \tag{10}$$

where $W(kR) = \frac{3(\sin kR - kR \cos kR)}{(kR)^3}$ and $R = (3M_h/4\pi\rho_m)^{1/3}$ with ρ_m denotes mean matter density of the Universe at present time. Hence σ_8 is variance of matter fluctuations in 8 Mpc h^{-1} which depends on model and galaxy bias [28]. Therefore, it is lead to define new parameter namely growth rate which depends on linear growth factor as:

$$f(a) \equiv \frac{d \ln D(a)}{d \ln a}. \tag{11}$$

As a result of this, the combination of two quantities, $f\sigma_8$ defined which is bias independent and could be measured by weak lensing and RSD [28].

2.3 Dynamical Dark Energy Models

The earliest dark energy model, the cosmological constant (Λ), satisfied the equation of state $w = -1$. It is constant and do not evolve during expansion history of the Universe. The mentioned problems of cosmological constant such as fine-tuning lead to propose dark energy models.

The main prediction of the dynamical models is the evolution of the dark energy density parameter. Combination of the matter and the dark energy density parameter predict expansion history of the Universe which is obtained as below:

$$H^2(z) = H_0^2[\Omega_m^0(1 + z)^3 + \Omega_{\mathrm{DE}}(z)]. \tag{12}$$

The dark energy density parameter expresses as:

$$\Omega_{\mathrm{DE}}(z) = \Omega_{\mathrm{DE}}^0 \Big[\int_0^z \frac{3(1 + w_{DE}(\tilde{z}))}{1 + \tilde{z}} d\tilde{z} \Big]. \tag{13}$$

If dark energy describes by ideal fluid with conserved energy-momentum tensor, then the dark energy equation of state can be considered as:

$$w(z) = \frac{P(z)}{\rho(z)}. \tag{14}$$

Independent of its physical origin, $w(z)$ effects on the expansion of the Universe and usually used to compare theoretical model predictions with observations [29].

Chavelier-Polarski-Linder (CPL) model is well-known and first proposed dynamical dark energy model, besides all benefit [30], it has divergence at $z \to -1$

Parameter	Prior
$\Omega_b h^2$	$[0.013, 0.033]$
$\Omega_c h^2$	$[0.010, 0.99]$
w_0	$[-1.035, -1.00]$
w_1	$[-0.05, 0.00]$
Θ_{MC}	$[0.50, 10.00]$
τ_{opt}	$[0.01, 0.80]$
n_s	$[0.70, 1.30]$
$\ln(10^{10} A_s)$	$[2.30, 5.0]$

Table 1: Priors on parameter space, used in the posterior analysis in this paper.

which causes unphysical future. Then, another parametrization for equation of state (EoS) was introduced by Feng et al [30] for DDE as:

$$w(z) = w_0 + w_1 \frac{z^2}{1 + z^2}. \tag{15}$$

which w_0 and w_1 are the free parameter of model. We consider the Feng model in this paper and its free parameters constraint with two data sets which reported in table 2. The model covers all CPL feature without divergence. In the next section, we report the data sets that we used for constrained the free parameters of the Feng and ΛCDM models for study H_0 and σ_8 tension.

3   Data Analysis

Several scientific projects have been established in order to assess desired observational accuracy for CMB and LSS and improve data analysis. Here we consider the last version of each data sets in order to analyze the tension in parameters value H_0 and σ_8 when constraints obtain from CMB and LSS data.

To constrain the models with observational data we consider prior ranges for parameters which are summarized in Table. 1. For constraints obtained from *Planck TT*+Pol+BAO we assumed that τ_{opt} is a free parameter. Since LSS data can not put tight constraints on τ_{opt} we fixed reionization optical depth with the value obtained from *Planck TT*+Pol+BAO data $\tau_{\mathrm{opt}} = 0.074$.
Parameter space in analysis with *Planck TT*+Pol+BAO includes the following parameters:

$$\{\Theta_p\} : \{w_0, w_1, \Omega_b h^2, \Omega_c h^2, H_0, \tau_{opt}, \mathcal{A}_s, n_s\}.$$

Then the reduced parameters space due to optical depth for WL+RSD reads as:

$$\{\Theta_p\} : \{w_0, w_1, \Omega_b h^2, \Omega_c h^2, H_0, \mathcal{A}_s, n_s\}.$$

Parameter	Feng TT+Pol+BAO	Feng WL+RSD	LCDM TT+Pol+BAO	LCDM WL+RSD
$\Omega_b h^2$	0.02211 ± 0.00016	$0.0241^{+0.0077}_{-0.0035}$	0.02211 ± 0.00016	0.045 ± 0.019
$\Omega_{\rm m}$	0.3128 ± 0.0072	$0.297^{+0.036}_{-0.032}$	0.3125 ± 0.0074	0.261 ± 0.030
w_0	$-1.0235^{+0.0053}_{+0.00012}$	$-1.019^{+0.010}_{-0.0093}$	-1.00	-1.00
w_1	$-0.038^{+0.018}_{-0.028}$	$-0.0271^{+0.0074}_{-0.020}$	0.00	0.00
$\Omega^0_{\rm DE}$	0.6872 ± 0.0072	$0.703^{+0.032}_{-0.036}$	0.6875 ± 0.0074	0.739 ± 0.030
H_0	67.40 ± 0.52	69.3 ± 4.3	67.42 ± 0.53	81^{+20}_{-10}
σ_8	$0.829^{+0.012}_{-0.0091}$	$0.756^{+0.051}_{-0.045}$	0.829 ± 0.013	0.762 ± 0.043
τ	$0.078^{+0.014}_{-0.011}$	Fix	$0.078^{+0.031}_{-0.031}$	Fix
$\ln(10^{10} A_s)$	$3.090^{+0.028}_{-0.021}$	$2.90^{+0.25}_{-0.51}$	3.090 ± 0.031	< 3.70
$\chi^2_{\rm CMB}$	11400	$-$	11404.4	$-$
$\chi^2_{\rm BAO}$	5.1	$-$	5.1	$-$
$\chi^2_{\rm RSD}$	$-$	4.5	$-$	5.3
$\chi^2_{\rm CFHTLENS}$	$-$	26.8	$-$	26.0

Table 2: The best fit of free parameters of DDE and LCDM models based on *Planck* TT+Pol+BAO and WL+RSD data in 68% confidence interval.

To find the best fit of given parameters by the mentioned data, we use maximum likelihood analysis. According to Bayesian statistics, the likelihood function given by:

$$\mathcal{L} = A \exp[-\chi^2/2], \qquad (16)$$

which A is constant and the value of χ^2 for combination of data and model with free parameters is:

$$\chi^2 = \sum_i \frac{1}{\sigma_i}[D_i - y(x|\mathcal{P})]^2. \qquad (17)$$

D_i refer to data points and $y(x|\mathcal{P})$ is model with free parameters. The best fit values are obtained by minimizing χ^2 or maximizing the likelihood.

To perform a maximum likelihood analysis we used the publicly available Monte Carlo Markov Chain code CosmoMC [31] which has been modified for the DDE model carefully. To obtain observational constraints, we used following data sets from early and late time Universe.

3.1 Early Time Universe Data Set

In order to obtain parameters constraints from early Universe, we consider Cosmic Microwave Background and Baryonic Acoustic Oscillations. Given data are uncorrelated and the total value of chi-square reads as:

$$\chi^2 = \chi^2_{CMB} + \chi^2_{BAO} \qquad (18)$$
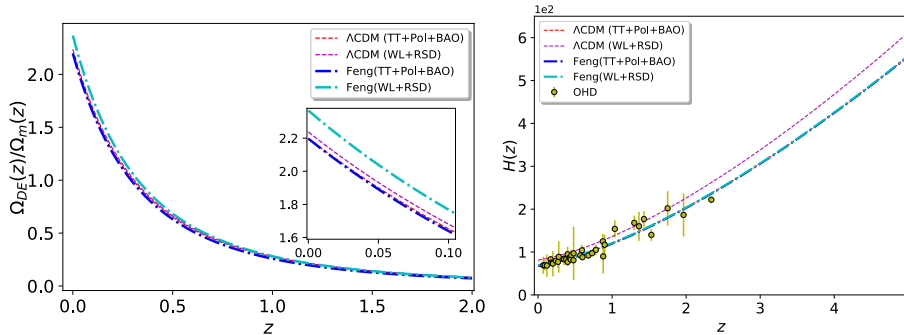
Figure 1: The left panel shows the ratio of dark energy to dark matter of models based on best fit for two data sets. The right panel exhibits the Hubble parameter of model and comparison with data versus redshift.

3.1.1   CMB

We use measurements of temperature anisotropies made by *Planck2015* which covers multi poles in the range of $\ell \approx 2 - 2500$ by using standard likelihood. Also to get tighter constraints we include polarization measurements by using polarization and temperature-polarization cross-correlation power spectra from *Planck 2015* data release [32].

3.1.2   BAO

We use Baryonic Acoustic Oscillations (BAO) measurements from the Six Degree Field Galaxy Survey (6dF)[33], the Main Galaxy Sample of Data Release 7 of Sloan Digital Sky Survey (SDSS-MGS) [34] and the LOWZ and CMASS galaxy samples of the Baryon Oscillation Spectroscopic Survey (BOSS-LOWZ and BOSS-CMASS, respectively) [35].

3.2   Late Time Universe Data Set

In order to obtain parameters constraints from late time Universe, we consider Weak Lensing and Redshift Space Distortion data. Given data are uncorrelated and the total value of chi-square reads as:

$$\chi^2 = \chi^2_{WL} + \chi^2_{RSD} \tag{19}$$

3.2.1   CFHTLenS

Gravitational lensing of photons by galaxies is a powerful tool to probe matter power spectrum and and variance of matter on $8 \; Mpc \; h^{-1}$ [32]. The coherent
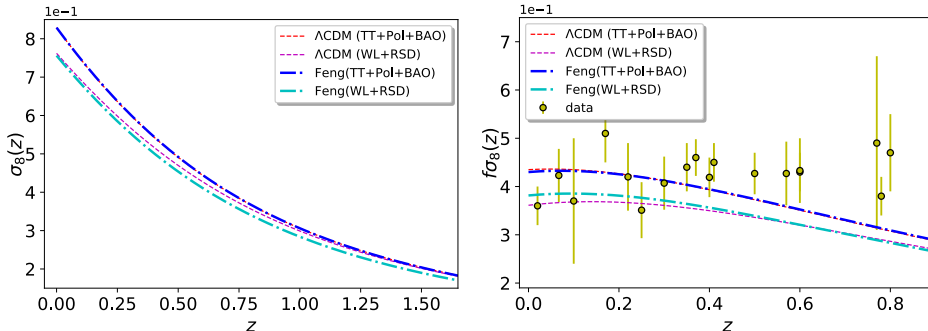
Figure 2: The left panel shows the variance of matter on $8\ Mpc\ h^{-1}$ for the models as a function of redshift and the right panel demonstrate $f\sigma_8$ consistency of the models and data versus redshift.

distortion of galaxies shape by large-scale structure, cosmic shear, is is an important way to constrain dark energy models due to its dependence to the growth of fluctuations and two scalar metric potentials. Cosmic shear measured by Canada France Hawaii Telescope Lensing Survey (CFHTLenS) [36] which is the largest weak lensing catalog. This is a 154 degree multi-color survey, optimized for weak lensing analyses, that spans redshifts ranging from $z \sim 0.2$ to $z \sim 1.3$. Here we consider the data subdivided into 6 redshift bins and we applied ultra-conservative cuts, that exclude ξ_- completely and cut the ξ_+ measurements at scales smaller than $\theta = 17'$ for all the tomographic redshift bins [39].

3.2.2   RSD

Non-linear effects can be measured by surveys of Redshift-Space Distortion (RSD) from peculiar velocities of galaxies within galaxy clusters. Peculiar velocities of galaxies distorts clustering pattern due to local inhomogeneities. On small scales, in the core of galaxy, clusters peculiar velocities are distributed randomly which lead to an effect called finger-of-god on redshift maps. However, on large scales, gravitation causes galaxies to fall into concentrations, so that velocity field is related to density field. In this paper, we use RSD measurements from BOSS CMASS-DR11 analyses of Samushia et al. (2014) [37]. The results of Samushia are expressed as a 3×3 covariance matrix for the three parameters D_V/r_{drag}, F_{AP} and $f\sigma_8$, evaluated at an effective redshift of $z_{\mathrm{eff}} = 0.57$, where F_{AP} is the Alcock-Paczynski parameter and D_V/r_{drag} is the distance ratio [32].

The best value of cosmological parameters for ΛCDM and Feng models by use of early and late time data sets base on likelihood analysis reported in table 2.
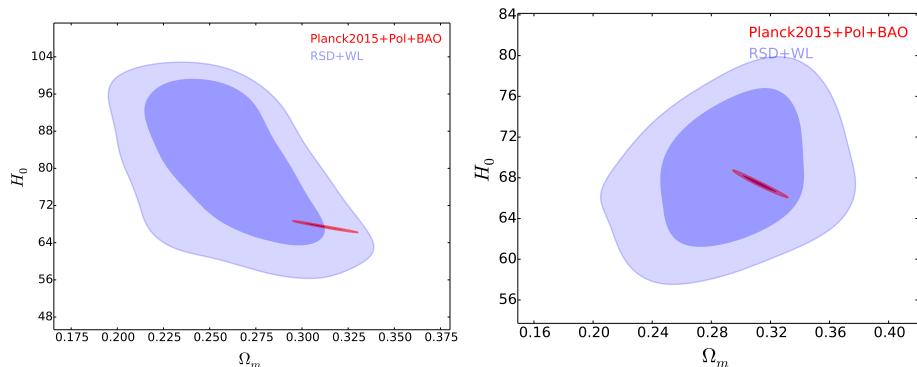
Figure 3: The left figure show ΛCDM model and right figures show for Feng model for $H_0 - \Omega_m$ two dimensional contour at 2σ confidence interval base on two data sets which the red one is for *Planck* TT+Pol+BAO and the violet one is for WL+RDS data.

4   Result and Discussion

Measurement from CMB and LSS can be used to constrain the cosmological parameters and other derived parameters such as Ω_m and σ_8 can be calculated but in ΛCDM model the value of H_0 and σ_8 show discrepancy and disagreement for CMB and LSS as early and late time data sets[18]. Therefore, we intend to discus effect of dynamical dark energy model on tension and investigate whether it reduces tension or not.

In contrast with CPL, the Feng model which considered in this paper is divergence free and cover all important feature of CPL [30]. The free parameters of ΛCDM and Feng models was obtained base on early and late data sets namely *Planck* TT+Pol+BAO and RSD+WL, at 1σ confidence interval which reported in table 2. In ΛCDM model, the value of $\Omega_m = 0.3125 \pm 0.0074$, $H_0 = 67.42 \pm 0.53$ and $\sigma_8 = 0.829 \pm 0.013$ for ΛCDM(*Planck* TT+Pol+BAO) and $\Omega_m = 0.261 \pm 0.030$, $H_0 = 81^{+20}_{-10}$ and $\sigma_8 = 0.762 \pm 0.04$ for ΛCDM(WL+RSD) did not overlap in two data sets with given error bars. Albeit, in the Feng model the value of $\Omega_m = 0.3128 \pm 0.0072$, $H_0 = 67.40 \pm 0.52$ in *Planck* TT+Pol+BAO and $\Omega_m = 0.297^{+0.036}_{-0.032}$, $H_0 = 69.3 \pm 4.3$ for WL+RSD cover each other in two data sets and σ_8 has still discrepancy. So, th best fit value for mentioned parameters demonstrate that dynamical dark energy could untie tension in H_0. Also, Zhao et al [38] shows that variable dark energy can improve tension on H_0.

Fig. 1,the left panel shows $\Omega_{\mathrm{DE}}/\Omega_{\mathrm{m}}$ of the models versus redshift, which exhibit the models with parameters base on late time are higher than early time and the Feng(WL+RSD) has higher value rather than ΛCDM(WL+RSD) models that
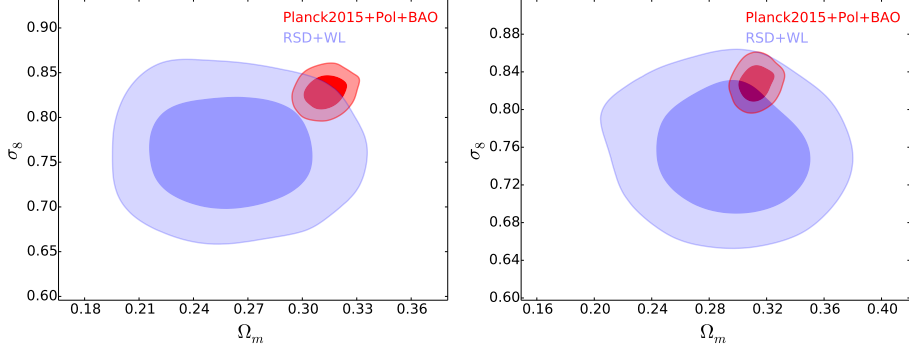
Figure 4: The left panel is for ΛCDM and the right panel is the Feng model for $\sigma_8 - \Omega_m$ two dimensional contour at 2σ confidence interval base on two data sets which the red one is for $Planck$ TT+Pol+BAO and the violet one is for WL+RDS data.

demonstrate the dynamical dark energy model is more powerful to suppress large scales structures. Right panel is H versus redshift compared with data. The ΛCDM(WL+RSD) is differ from others due to its present time value, $H_0 = 81^{+20}_{-10}$, which is higher that the others but the models are not distinguishable in the given error bars. The values H_0 for both data sets in ΛCDM model show the discrepancy.

Fig 2, the left panel is the amplitude of mass fluctuations in 8 $Mpch^{-1}$ versus redshift. The Feng (WL+RSD) produce lower value for σ_8 due to higher density value of dark energy mentioned in left panel of fig 1 in contrast with Feng($Planck$ TT+Pol+BAO) and the ΛCDM follow DDE model in both data set. therefore it causes lower value in $f\sigma_8$ which demonstrates in fig 2. The right panel of fig 2 shows liner growth of fluctuation for mentioned models which checked by observational data. The models base on two data sets are not distinguishable in $z < 0.4$ red shift bin with given error bars albeit for $z > 0.4$ the models show different behavior rather than the $f\sigma_8$ data. So it is indicate that the Feng model could not completely alleviate σ_8 tension.

In fig 3 from left to right panel present respectively ΛCDM and Feng models $H_0 - \Omega_m$ two dimensional contour plot at 1 and 2σ confidence interval level which the red one is for $Planck$ TT+Pol+BAO and the violet one is for WL+RDS data. Plots demonstrate in ΛCDM model the early and late time data are disagreement for H_0 value but considering Feng model as dynamical dark energy model rather than ΛCDM model causes that the tension completely disappear from 2σ to 1σ region in $H_0 - \Omega_m$ parameters.

Fig 4 exhibits $\sigma_8 - \Omega_m$ parameters at 1 and 2σ confidence interval for two data sets. The left panel is ΛCDM and the right panel is Feng model. In ΛCDM model WL+RSD and $Planck$ TT+Pol+BAO are completely separated at 1σ but

including Feng model (righ panel) lead to two data set touch each other at 1σ confidence level. Hence, dynamical dark energy model decrease the $\sigma_8 - \Omega_m$ tension in compare with ΛCDM model almost 1σ but the tension does not disappear completely.

5   Conclusion

In this research, we consider the Feng and ΛCDM models in order to study the discrepancy H_0 and σ_8 value between early and late time data sets. So, we utilize the last version of mentioned data to obtain free parameters of model. The early Universe data consist CMB from *Planck 2015* and BAO from 6dF data. The late time data include RSD from BOSS CMASS DR11 and WL from CFHTLenS data. we obtain $\Omega_{\mathrm{DE}} = 0.6875 \pm 0.0074$, $\Omega_{\mathrm{m}} = 0.3125 \pm 0.0074$, $H_0 = 67.42 \pm 0.53$ and $\sigma_8 = 0.829 \pm 0.013$ for $\Lambda CDM(Planck$ TT+Pol+BAO) and $\Omega_{\mathrm{DE}} = 0.739 \pm 0.030$, $\Omega_{\mathrm{m}} = 0.261 \pm 0.030$, $H_0 = 81^{+20}_{-10}$ and $\sigma_8 = 0.762 \pm 0.04$ for $\Lambda CDM(\mathrm{WL+RSD})$ respectively.

Furthermore for the Feng(*Planck* TT+Pol+BAO) model $\Omega_{\mathrm{DE}} = 0.6872 \pm 0.0072$, $\Omega_{\mathrm{m}} = 0.3128 \pm 0.0072$, $H_0 = 67.40 \pm 0.52$ and $\sigma_8 = 0.829^{+0.012}_{-0.0091}$ and for the Feng(WL+RSD) model $\Omega_{\mathrm{DE}} = 0.703^{+0.032}_{-0.036}$, $\Omega_{\mathrm{m}} = 0.297^{+0.036}_{-0.032}$, $H_0 = 69.3 \pm 4.3$ and $\sigma_8 = 0.756^{+0.051}_{-0.045}$ acquired at 1σ confidence interval respectively.

In ΛCDM model, the best value of Ω_m, H_0 and σ_8 does not cover each other in late and early data set at 1σ confidence interval while the Feng model the value of Ω_m and H_0 are completely in agreement with two data sets. Although the discrepancy remained for σ_8 parameter.

According fig 1 and 2, the Feng(WL+RSD) produces more value for $\Omega_{\mathrm{DE}}/\Omega_{\mathrm{m}}$ and it causes lower value for σ_8 and $f\sigma_8$ in contrast with the Feng (*Planck* TT+Pol+BAO). This behavior is weakly seen in ΛCDM model which is because of late time domination of dark energy but among the model, Feng is more powerful in expanding the Universe. the DDE and ΛCDM models base on early time data are more compatible with $f\sigma_8$ data, although for $z > 0.4$ the models and data behave differently which show that dark energy could not fully solve the σ_8 tension.

Dynamical dark energy is totally figuring out the H_0 tension [41]. In fig 3 shows that in Feng model the H_0 tension between two data sets disappeared.

It is shown that massive neutrino decreases σ_8 tension from 2.5σ to 1.6σ [18] and also we demonstrate in fig 4 that Feng model as a dynamical dark energy model could improve the mentioned tension from 2σ to 1σ region. Hence the combination of massive neutrino plus dark energy to study σ_8 tension between early and late time data left for next work.

Conflicts of Interest. The authors declare that there are no conflicts of interest regarding the publication of this article.

References

[1] J. Martin, Everything You Always Wanted To Know About The Cosmological Constant Problem (But Were Afraid To Ask), Comptes Rendus Physique **13** (2012) $566 - 665$.

[2] R. R. Caldwell and E. V. Linder, Limits of quintessence, Phys. Rev. Lett. **95** (2005) 141301.

[3] C. Armendariz-Picon, V. F. Mukhanov and P. J. Steinhardt, Essentials of k-essence, Phys. Rev. D **63** (2001) 103510.

[4] R. R. Caldwell, A phantom menace? Cosmological consequences of a dark energy component with super-negative equation of state, Phys. Lett. B **545** (2002) $23 - 29$.

[5] L. Amendola, Coupled quintessence, Phys. Rev. D **62** (2000) 043511.

[6] J. S. Peracaula, J. d. Cruz Pérez and A. Gómez-Valent, Dynamical dark energy vs. $\Lambda = $ const in light of observations, Europhysics Letters **121** (2018) 043511.

[7] S. M. Carroll, V. Duvvuri, M. Trodden and M. S. Turner, Is cosmic speed - up due to new gravitational physics?, Phys. Rev. D **70** (2004) 043528.

[8] S. Nojiri and S. D. Odintsov, Modified gravity with negative and positive powers of the curvature: Unification of the inflation and of the cosmic acceleration, Phys. Rev. D **68** (2003) 123512.

[9] L. Amendola, Scaling solutions in general nonminimal coupling theories, Phys. Rev. D **60** (1999) 043501.

[10] J. P. Uzan, Cosmological scaling solutions of nonminimally coupled scalar fields, Phys. Rev. D **59** (1999) 123510.

[11] P. S. Corasaniti, B. A. Bassett, C. Ungarelli and E. J. Copeland, Model - independent dark energy differentiation with the ISW effect, Phys. Rev. Lett. **90** (2003) 091303.

[12] Y. S. Song and W. J. Percival, Reconstructing the history of structure formation using Redshift Distortions, JCAP **0910** (2009) 004.

[13] N. Kaiser, Clustering in real space and in redshift space, Mon. Not. Roy. Astron. Soc. **227** (1987) $1 - 21$.

[14] D. Huterer and D. L. Shafer, Dark energy two decades after: Observables, probes, consistency tests, Rept. Prog. Phys. **81** (1) (2018) 016901.

[15] S. Basilakos, The growth index of matter perturbations using the clustering of dark energy, Mon. Not. Roy. Astron. Soc. **449** (2) (2015) $2151 - 2155$.

[16] H. Hoekstra and B. Jain, Weak Gravitational Lensing and its Cosmological Applications, Ann. Rev. Nucl. Part. Sci. **58** (2008) $99 - 123$.

[17] N. MacCrann, J. Zuntz, S. Bridle, B. Jain and M. R. Becker, Cosmic Discordance: Are Planck CMB and CFHTLenS weak lensing measurements out of tune?, Mon. Not. Roy. Astron. Soc. **451** (3) (2015) $2877 - 2888$.

[18] R. A. Battye, T. Charnock and A. Moss, Tension between the power spectrum of density perturbations measured on large and small scales, Phys. Rev. D **91** (10) (2015) 103508.

[19] A. Gomez-Valent and J. Sola, Relaxing the σ_8-tension through running vacuum in the Universe, EPL **120** (3) (2017) 39001.

[20] T. Charnock, R. A. Battye and A. Moss, Planck data versus large scale structure : Methods to quantify discordance, Phys. Rev. D **95** (12) (2017) 123535.

[21] J. Lesgourgues, G. Marques-Tavares and M. Schmaltz, Evidence for dark matter interactions in cosmological precision data?, JCAP **1602** (2) (2016) 037.

[22] T. Bringmann, F. Kahlhoefer, K. Schmidt-Hoberg and P. Walia, Converting nonrelativistic dark matter to radiation, Phys. Rev. D **98** (2) (2018) 023543.

[23] D. Sapone, M. Kunz and M. Kunz, Fingerprinting Dark Energy, Phys. Rev. D **80** (2009) 083519.

[24] C. P. Ma and E. Bertschinger, Cosmological perturbation theory in the synchronous and conformal Newtonian gauges, Astrophys. J. **455** (1995) $7 - 25$.

[25] A. Meiksin and M. White The growth of correlations in the matter power spectrum, Mon. Not. Roy. Astron. Soc. **308** (1999) 1179.

[26] A. Pouri, S. Basilakos and M. Plionis, Precision growth index using the clustering of cosmic structures and growth data, JCAP **1408** (2014) 042.

[27] Coles, Peter, and Francesco Lucchin. Cosmology: The origin and evolution of cosmic structure. John Wiley and Sons, 2003.

[28] Y. S. Song and W. J. Percival, Reconstructing the history of structure formation using Redshift Distortions, JCAP **0910** (2009) 004.

[29] S. Nesseris and L. Perivolaropoulos, Comparison of the legacy and gold SNIa dataset constraints on dark energy models, Phys. Rev. D **72** (2005) 123519.

[30] C. J. Feng, X. Y. Shen, P. Li and X. Z. Li, A New Class of Parametrization for Dark Energy without Divergence, JCAP **1209** (2012) 023.

[31] A. Lewis and S. Bridle, Cosmological parameters from CMB and other data: A Monte Carlo approach, Phys. Rev. D **66** (10) (2002) $103511 - 103516$.

[32] P. A. R. Ade, N. Aghanim, M. Arnaud, M. Ashdown, J. Aumont, C. Baccigalupi, A. J. Banday, R. B. Barreiro, J. G. Bartlett, N. Bartolo, E. Battaner, R. Battye, K. Benabed, A. Benoit, A. Benoit-Levy, J. -P. Bernard, M. Bersanelli, P. Bielewicz, J. J. Bock, A. Bonaldi, L. Bonavera, J. R. Bond, J. Borrill, F. R. Bouchet, F. Boulanger, M. Bucher, C. Burigana, R. C. Butler, E. Calabrese, J.-F. Cardoso, A. Catalano, A. Challinor, A. Chamballu, R. -R. Chary, H. C. Chiang, J. Chluba, P. R. Christensen, S. Church, D. L. Clements, S. Colombi, L. P. L. Colombo, C. Combet, A. Coulais, B. P. Crill, A. Curto, F. Cuttaia, L. Danese, R. D. Davies, R. J. Davis, P. de Bernardis, A. de Rosa, G. de Zotti, J. Delabrouille, F. -X. Desert, E. Di Valentino, C. Dickinson, J. M. Diego, K. Dolag, H. Dole, S. Donzelli, O. Dore, M. Douspis, A. Ducout, J. Dunkley, X. Dupac, G. Efstathiou, F. Elsner, T. A. Ensslin, H. K. Eriksen, M. Farhang, J. Fergusson, F. Finelli, O. Forni, M. Frailis, A. A. Fraisse, E. Franceschi, A. Frejsel, S. Galeotta, S. Galli, K. Ganga, C. Gauthier, M. Gerbino, T. Ghosh, M. Giard, Y. Giraud-Heraud, E. Giusarma, E. Gjerlow, J. Gonzalez-Nuevo, K. M. Gorski, S. Gratton, A. Gregorio, A. Gruppuso, J. E. Gudmundsson, J. Hamann, F. K. Hansen, D. Hanson, D. L. Harrison, G. Helou, S. Henrot-Versille , C. Hernandez-Monteagudo, D. Herranz, S. R. Hildebrandt, E. Hivon, M. Hobson, W. A. Holmes, A. Hornstrup, W. Hovest, Z. Huang, K. M. Huffenberger, G. Hurier, A. H. Jaffe, T. R. Jaffe, W. C. Jones, M. Juvela, E. Keihanen, R. Keskitalo, T. S. Kisner, R. Kneissl, J. Knoche, L. Knox, M. Kunz, H. Kurki-Suonio, G. Lagache, A. Lahteenmaki, J. -M. Lamarre, A. Lasenby, M. Lattanzi, C. R. Lawrence, J. P. Leahy, R. Leonardi, J. Lesgourgues, F. Levrier, A. Lewis, M. Liguori, P. B. Lilje, M. Linden-Vornle, M. Lopez-Caniego, P. M. Lubin, J. F. Macias-Perez, G. Maggio, D. Maino, N. Mandolesi, A. Mangilli, A. Marchini, P. G. Martin, M. Martinelli, E. Martinez-Gonzalez, S. Masi, S. Matarrese, P. Mazzotta, P. McGehee, P. R. Meinhold, A. Melchiorri, J. -B. Melin, L. Mendes, A. Mennella, M. Migliaccio, M. Millea, S. Mitra, M. -A. Miville-Deschenes, A. Moneti, L. Montier, G. Morgante, D. Mortlock, A. Moss, D. Munshi, J. A. Murphy, P. Naselsky, F. Nati, P. Natoli, C. B. Netterfield, H. U. Norgaard-Nielsen, F. Noviello, D. Novikov, I. Novikov, C. A. Oxborrow, F. Paci, L. Pagano, F. Pajot, R. Paladini, D. Paoletti, B. Partridge, F. Pasian, G. Patanchon, T. J. Pearson, O. Perdereau, L. Perotto, F. Perrotta, V. Pettorino, F. Piacentini, M. Piat, E. Pierpaoli, D. Pietrobon, S. Plaszczynski, E. Pointecouteau, G. Polenta, L. Popa, G. W. Pratt, G. Prezeau, S. Prunet, J. -L. Puget, J. P.

Rachen, W. T. Reach, R. Rebolo, M. Reinecke, M. Remazeilles, C. Renault, A. Renzi, I. Ristorcelli, G. Rocha, C. Rosset, M. Rossetti, G. Roudier, B. Rouille d'Orfeuil, M. Rowan-Robinson, J. A. Rubino-Martin, B. Rusholme, N. Said, V. Salvatelli, L. Salvati, M. Sandri, D. Santos, M. Savelainen, G. Savini, D. Scott, M. D. Seiffert, P. Serra, E. P. S. Shellard, L. D. Spencer, M. Spinelli, V. Stolyarov, R. Stompor, R. Sudiwala, R. Sunyaev, D. Sutton, A. -S. Suur-Uski, J. -F. Sygnet, J. A. Tauber, L. Terenzi, L. Toffolatti, M. Tomasi, M. Tristram, T. Trombetti, M. Tucci, J. Tuovinen, M. Turler, G. Umana, L. Valenziano, J. Valiviita, B. Van Tent, P. Vielva, F. Villa, L. A. Wade, B. D. Wandelt, I. K. Wehus, M. White, S. D. M. White, A. Wilkinson, D. Yvon, A. Zacchei, A. Zonca, Planck 2015 results. XIII. Cosmological parameters, Astron. Astrophys. **594** (2016) A13.

[33] F. Beutler, C. Blake, M. Colless, D. H. Jones, L. Staveley-Smith, L. Campbell, Q. Parker, W. Saunders, F. Watson, The 6dF Galaxy Survey: Baryon Acoustic Oscillations and the Local Hubble Constant, Mon. Not. Roy. Astron. Soc. **416** (2011) $3017 - 3032$.

[34] A. J. Ross, L. Samushia, C. Howlett, W. J. Percival, A. Burden and M. Manera, The clustering of the SDSS DR7 main Galaxy sample I. A 4 per cent distance measure at $z = 0.15$, Mon. Not. Roy. Astron. Soc. **449** (1) (2015) $835 - 847$.

[35] L. Anderson, E. Aubourg, S. Bailey, F. Beutler, V. Bhardwaj, M. Blanton, A. S. Bolton, J. Brinkmann, J. R. Brownstein, A. Burden, C. -H. Chuang, A. J. Cuesta, K. S. Dawson, D. J. Eisenstein, S. Escoffier, J. E. Gunn, H. Guo, S. Ho, K. Honscheid, C. Howlett, D. Kirkby, R. H. Lupton, M. Manera, C. Maraston, C. K. McBride, O. Mena, F. Montesano, R. C. Nichol, S. E. Nuza, M. D. Olmstead, N. Padmanabhan, N. Palanque-Delabrouille, J. Parejko, W. J. Percival, P. Petitjean, F. Prada, A. M. Price-Whelan, B. Reid, N. A. Roe, A. J. Ross, N. P. Ross, C. G. Sabiu, S. Saito, L. Samushia, A. G. Sanchez, D. J. Schlegel, D. P. Schneider, C. G. Scoccola, H. -J. Seo, R. A. Skibba, M. A. Strauss, M. E. C. Swanson, D. Thomas, J. L. Tinker, R. Tojeiro, M. V. Magana, L. Verde, D. A. Wake, B. A. Weaver, D. H. Weinberg, M. White, X. Xu, C. Yeche, I. Zehavi, G, -B. Zhao, The clustering of galaxies in the SDSS-III Baryon Oscillation Spectroscopic Survey: baryon acoustic oscillations in the Data Releases 10 and 11 Galaxy samples, Mon. Not. Roy. Astron. Soc. **441** (1) (2014) $24 - 62$.

[36] T. Erben, H. Hildebrandt, L. Miller, L. van Waerbeke, C. Heymans, H. Hoekstra, T. D. Kitching, Y. Mellier, J. Benjamin, C. Blake, C. Bonnett, O. Cordes, J. Coupon, L. Fu, R. Gavazzi, B. Gillis, E. Grocutt, S. D. J. Gwyn, K. Holhjem, M. J. Hudson, M. Kilbinger, K. Kuijken, M. Milkeraitis, B. T. P. Rowe, T. Schrabback, E. Semboloni, P. Simon, M. Smit, O. Toader, S. Vafaei, E. van Uitert, M. Velander, CFHTLenS: The Canada-France-Hawaii Telescope Lensing Survey, Mon. Not. Roy. Astron. Soc. **427** (2012) $146 - 166$.

[37] L. Samushia, B. A. Reid, M. White, W. J. Percival, A. J. Cuesta, L. Lombriser, M. Manera, R. C. Nichol, D. P. Schneider, D. Bizyaev, H. Brewington, E. Malanushenko, V. Malanushenko, D. Oravetz, K. Pan, A. Simmons, A. Shelden, S. Snedden, J. L. Tinker, B. A. Weaver, D. G. York, G. -B. Zhao, The Clustering of Galaxies in the SDSS-III DR9 Baryon Oscillation Spectroscopic Survey: Testing Deviations from Λ and General Relativity using anisotropic clustering of galaxies, Mon. Not. Roy. Astron. Soc. **429** (2013) $1514 - 1528$.

[38] G. -B. Zhao, M. Raveri, L. Pogosian, Y. Wang, R. G. Crittenden, W. J. Handley, W. J. Percival, F. Beutler, J. Brinkmann, C. -H. Chuang, A. J. Cuesta, D. J. Eisenstein, F. -S. Kitaura, K. Koyama, B. L'Huillier, R. C. Nichol, M. M. Pieri, S. Rodriguez-Torres, A. J. Ross, G. Rossi, A. G. Sánchez, A. Shafieloo, J. L. Tinker, R. Tojeiro, J. A. Vazquez, H. Zhang, Dynamical dark energy in light of the latest observations, Nat. Astron. **1** (9) (2017) $627 - 632$.

[39] J. Benjamin, L. V. Waerbeke, C. Heymans, M. Kilbinger, T. Erben, H. Hildebrandt, H. Hoekstra, T. D. Kitching, Y. Mellier, L. Miller, B. Rowe, T. Schrabback, F. Simpson, J. Coupon, L. Fu, J. Harnois-Déraps, M. J. Hudson, K. Kuijken, E. Semboloni, S. Vafaei, M. Velander, CFHTLenS tomographic weak lensing: Quantifying accurate redshift distributions, Mon. Not. Roy. Astron. Soc. **431** (2013) 1547.

[40] C. Heymans, E. Grocutt, A. Heavens, M. Kilbinger, T. D. Kitching, F. Simpson, J. Benjamin, T.s Erben, H. Hildebrandt, H. Hoekstra, Y. Mellier, L. Miller, L. Van Waerbeke, M. L. Brown, J. Coupon, L. Fu, J. Harnois-Deraps, M. J. Hudson, K. Kuijken, B. Rowe, T. Schrabback, E. Semboloni, S. Vafaei, M. Velander, CFHTLenS tomographic weak lensing cosmological parameter constraints: Mitigating the impact of intrinsic galaxy alignments, Mon. Not. Roy. Astron. Soc. **432** (2013) $2433 - 2453$.

[41] A. S. Ebrahimi, M. Monemzadeh and H. Moshafi, Are Cold Dynamical Dark Energy Models Distinguishable in the Light of the Data?, (2018). `arXiv:1802.05087`.

Aghile Sadat Ebrahimi
Department of Physics,
University of Kashan,
Kashan, I. R. Iran
e-mail: aghileh.ebrahimi@gmail.com

Majid Monemzadeh
Department of Physics,
University of Kashan,
University of Kashan,

Kashan, I. R. Iran
e-mail: monem@kashanu.ac.ir

Hossein Moshafi
Ibn-Sina Laboratory,
Shahid Beheshti University,
Velenjak,Tehran, I. R. Iran
e-mail: hosseinmoshafi@gmail.com

Seyed Mohammad Sadegh Movahed
Department of physics,
shahid Beheshti University,
Velenjak,Tehran, I. R. Iran
e-mail: m.s.movahed@ipm.ir